

## First-principles calculation of impurity-solution energies in Cu and Ni

B. Drittler

*Institut für Festkörperforschung der Kernforschungsanlage Jülich, D-5170 Jülich, Federal Republic of Germany*

M. Weinert

*Department of Physics, Brookhaven National Laboratory, Upton, New York 11973*

R. Zeller and P. H. Dederichs

*Institut für Festkörperforschung der Kernforschungsanlage Jülich, D-5170 Jülich, Federal Republic of Germany*

(Received 3 August 1988)

We present *ab initio* calculations for the solution energies of *3d* impurities in Cu and Ni hosts. The calculations are based on density-functional theory and the KKR Green's-function method. We apply a grand-canonical energy functional which is extremal against non-particle-conserving charge variations and give an extension of Lloyd's formula for complex energies. The full nonsphericity of the charge density is used in the double counting terms. Test calculations show that it is sufficient to take the perturbation of one shell of host atoms around the impurity into account. The calculated solution energies of *3d* impurities in Cu and Ni are in good agreement with the experimental data and with the values predicted by Miedema's model.

### I. INTRODUCTION

Solution energies of impurities are the most important properties determining the energetics of dilute alloys. This paper aims at calculating these quantities on an *ab initio* basis using density-functional theory. Whereas total-energy calculations for ordered alloys are nowadays standard, reliable calculations for dilute alloys or even concentrated disordered alloys are considerably more difficult. The basic problem is the loss of translation invariance so that band-structure methods cannot be applied. In the dilute limit, Green's-function methods<sup>1-4</sup> offer a convenient and elegant way to solve the inhomogeneous problem of a single impurity in an otherwise ideal crystal. For impurities in transition metals only model calculations of the solution energies based on the tight-binding method have been performed up to now.<sup>5-7</sup>

Our calculations apply the Korringa-Kohn-Rostoker (KKR) Green's-function method<sup>2,3</sup> which has been developed in our group. This method relies on two basic assumptions: (i) In each cell the atomic potentials are approximated by spherical potentials of muffin-tin or atomic-sphere form; (ii) the potential perturbation is localized in the vicinity of the defect. Extensive calculations<sup>3</sup> have shown that the latter assumption is not at all serious if only the local properties of the defect are of concern. Here we will show that for a reliable calculation of solution energies in fcc crystals it is sufficient to include the potential perturbation of the impurity and the first shell of neighbors only. For the potentials we assume an atomic sphere rather than a muffin-tin form. The slight inaccuracies introduced by the overlapping of the potentials should be more than balanced by the better space filling of the Wigner-Seitz spheres.<sup>4</sup> In addition to the above approximation we also assume (iii) that lattice relaxations around the impurity can be neglected. This limits our calculations to systems with not too large size

misfits. Due to the neglect of lattice relaxations our calculated solution energies should always be somewhat too high.

The general formalism of the total-energy calculations is described in Sec. II. The basic strategy is to exploit the extremal properties of the total energy to the largest possible extent. For instance, the spherical Wigner-Seitz potentials are only used to generate the wave functions and the charge densities, whereas the full nonsphericity of the charge density is used to calculate the double-counting contributions, i.e., both the Coulomb as well as the exchange-correlation terms. This is achieved by using a multipole expansion of the charge density and the potential. All integrals over the Wigner-Seitz cells are replaced by integrals over Wigner-Seitz spheres. Since the Friedel sum rule cannot be satisfied exactly in the calculation, we introduce a grand-canonical energy functional which is also extremal against non-particle-conserving trial solutions. The single-particle energies are calculated by Lloyd's formula<sup>8</sup> in the adaption of Lehmann.<sup>9</sup> By taking advantage of the analytical properties of the Green's function, we calculate the charge density as well as the single-particle energies by a contour integration in the complex energy plane.<sup>10-12</sup> Thus the Kohn-Sham equations are only solved for complex energies. This leads to problems in the application of Lloyd's formula in its traditional form<sup>9</sup> since the phase shifts  $\delta_l(E)$  occurring in this formula are nonanalytical for complex energies. Therefore, in the Appendix we derive a proper generalization of Lloyd's formula having the desired analytical behavior for complex energies.

In Sec. III we present test calculations for V impurities in Cu. We discuss particularly the convergence of the solution energies by adding up to four shells of perturbed neighbor potentials to the calculation. We also discuss the convergence with respect to the maximal angular momentum  $l_{\max}$  used in the expansions for the wave

functions and charge densities. In Sec. IV we present results for 3d impurities in Cu and Ni hosts. These systems are very different in so far as 3d impurities show an endothermic solubility in Cu but an exothermic solubility in Ni. We discuss the importance of magnetic effects and the reliability of the single-site approximation, which forms the basis of KKR CPA (coherent-potential approximation) calculations for concentrated alloys. By comparing our results with experimental values as well as values predicted by Miedema's model<sup>13</sup> we find that the experimental trends are reproduced and that the agreement is gratifying.

$$G(\mathbf{r}+\mathbf{R}^n, \mathbf{r}'+\mathbf{R}^{n'}; E) = \sqrt{E} \delta_{nn'} \sum_L Y_L(\mathbf{r}) H_L^n(r_>; E) R_L^n(r_<; E) Y_L(\mathbf{r}') + \sum_{L, L'} Y_L(\mathbf{r}) R_L^n(r; E) G_{LL'}^{nn'}(E) R_{L'}^{n'}(r'; E) Y_{L'}(\mathbf{r}'). \quad (1)$$

Here the vectors  $\mathbf{r}$  and  $\mathbf{r}'$  are restricted to the Wigner-Seitz cell and  $r_>$  ( $r_<$ ) denotes the larger (smaller) value of  $r=|\mathbf{r}|$  and  $r'=|\mathbf{r}'|$ . The subscript  $L=(l, m)$  denotes angular-momentum numbers and  $Y_L(\mathbf{r})$  are real spherical harmonics. The regular  $[R_L^n(r; E)]$  and irregular solutions  $[H_L^n(r, E)]$  of the radial Schrödinger equation for the  $n$ th muffin-tin potential are defined by their asymptotic behavior outside the muffin-tin sphere of radius  $S$ , for  $r \geq S$

$$\begin{aligned} R_L^n(r; E) &= j_l(\sqrt{E}r) + \sqrt{E} t_l^n(E) h_l(\sqrt{E}r), \\ H_L^n(r; E) &= h_l(\sqrt{E}r), \end{aligned} \quad (2)$$

where  $j_l$  and  $h_l$  are the spherical Bessel and Hankel functions and  $t_l^n(E)$  is the usual on-shell  $t$  matrix for the  $n$ th potential.

All the information about the multiple scattering between the muffin tins is contained in the structural Green's-function matrix  $G_{LL'}^{nn'}(E)$ . It can be related to its counterpart  $\hat{G}_{LL'}^{nn'}(E)$  for the host crystal by an algebraic Dyson equation:

$$G_{LL'}^{nn'}(E) = \hat{G}_{LL'}^{nn'}(E) + \sum_{n'', L''} \hat{G}_{LL''}^{nn''}(E) \Delta t_{l''}^{n''}(E) G_{L''L'}^{n''n'}(E). \quad (3)$$

The summation goes over all sites  $n''$  and angular momenta  $L''$  for which the perturbation  $\Delta t_{l''}^{n''}(E) = t_{l''}^{n''}(E) - \hat{t}_{l''}^{n''}(E)$  of the  $t$  matrices  $\hat{t}$  of the host is significant. Typically we include angular momenta up to  $l=3$  and a few shells of perturbed host potentials around the impurity. The Dyson equation is solved using a group-theoretical decomposition into irreducible submatrices, which considerably reduces the computer time.

The charge density is obtained from the Green's function by

$$n(\mathbf{r}) = -\frac{2}{\pi} \int^{E_F} dE \operatorname{Im} G(\mathbf{r}, \mathbf{r}; E) = -\frac{2}{\pi} \operatorname{Im} \oint dz G(\mathbf{r}, \mathbf{r}; z). \quad (4)$$

## II. THEORETICAL METHOD

### A. Solution of the Kohn-Sham equations

Our calculations are based on multiple-scattering theory using the KKR-Green's-function method, which we will outline shortly for paramagnetic systems; the generalization to magnetic systems is obvious (Ref. 3). For a lattice of muffin-tin potentials centered at positions  $\mathbf{R}^n$  the Green's function can be expanded into eigensolutions of these spherically symmetric local potentials:

Since the Green's function is, as a function of the complex energy variable  $z$ , analytical on the whole physical sheet with the exception of the real axis, the energy integral can be transformed to a contour integral in the complex energy plane,<sup>10-12</sup> provided this contour ends at the Fermi energy  $E_F$  on the real axis. The contour integral can be very easily calculated with rather few energy points since for complex energies  $z$  the Green's function is rather structureless. In practice this means an enormous saving of computer time.<sup>11</sup>

In the calculations we employ density-functional theory in the local-density approximation of von Barth and Hedin<sup>4</sup> but with the parameters as determined by Moruzzi *et al.*<sup>15</sup> All potentials are calculated self-consistently by an iteration technique. One problem worth discussing in some detail is connected with the jump of the potential at the muffin-tin or Wigner-Seitz radius. In solving the radial Schrödinger equation, e.g., by Numerov's or an equivalent method, one has to choose a certain radial mesh. The errors of the wave functions vary with a high power of the mesh size  $\delta$ , e.g.,  $\sim \delta^5$ , provided the potential is smoothly varying. On the other hand, large errors are introduced if one integrates over the region of the potential jump. This however is not necessary since the wave function outside is known analytically. For instance, in calculating the  $t$  matrix one needs the logarithmic derivative of the radial wave function at the muffin-tin or Wigner-Seitz boundary. This can be obtained by extrapolating from inside to the boundary so that no numerically calculated values outside the boundary are needed.

### B. Extremal properties of the total energy

It is well known that the total energy  $E\{n(\mathbf{r})\}$ , given as the sum of the kinetic energy  $T_s\{n(\mathbf{r})\}$ , the Coulomb energy  $U\{n(\mathbf{r})\}$ , and the exchange-correlation part  $E_{xc}\{n(\mathbf{r})\}$ ,

$$E\{n(\mathbf{r})\} = T_s\{n(\mathbf{r})\} + U\{n(\mathbf{r})\} + E_{xc}\{n(\mathbf{r})\}, \quad (5)$$

is extremal against charge variations  $\delta n(\mathbf{r})$  around the ground-state density. From the equation

$$\delta E = \int d\mathbf{r} \frac{\delta E}{\delta n(\mathbf{r})} \delta n(\mathbf{r}) = E_F \int d\mathbf{r} \delta n(\mathbf{r})$$

one sees that  $\delta E$  vanishes, if  $\int d\mathbf{r} \delta n(\mathbf{r}) = 0$ , i.e., as long as the trial charge density  $n(\mathbf{r})$  gives the correct particle number  $N = \int d\mathbf{r} n(\mathbf{r})$ . Contrary to the usual band-structure methods where  $E_F$  is adjusted to yield charge neutrality, this cannot be achieved in point-defect calculations since the Fermi energy is fixed by the host. In metals perfect screening can only occur if an infinitely long-ranged perturbation potential is allowed. The violation of charge neutrality is typically 0.1 or 0.01 electrons, if one or four shells of perturbed neighboring potentials are included. This problem can be avoided, if the generalized functional  $\tilde{E}\{n(\mathbf{r})\}$ ,<sup>16</sup>

$$\tilde{E}\{n(\mathbf{r})\} = E\{n(\mathbf{r})\} - E_F \left[ \int n(\mathbf{r}) d\mathbf{r} - N \right], \quad (6)$$

is considered. Clearly

$$\delta \tilde{E} = \int d\mathbf{r} \left[ \frac{\delta E}{\delta n(\mathbf{r})} - E_F \right] \delta n(\mathbf{r}) = 0 \quad (7)$$

vanishes for general, i.e., also for non-particle-conserving, variations  $\delta n(\mathbf{r})$ . Physically this corresponds to the transition to a grand-canonical functional, for which the chemical potential rather than the particle number  $N$  is the basic variable. One can also understand the correction in Eq. (6) such that the missing charge  $\Delta N = N - \int n(\mathbf{r}) d\mathbf{r}$  is added far away from the impurity at the Fermi level of the host giving an additional energy contribution  $E_F \Delta N$ .

It is noteworthy that the grand-canonical functional  $\tilde{E}\{n(\mathbf{r})\}$  does not depend on the choice of the zero-energy level, as can be easily shown. A change of the energy scale by  $V_0$ , which can be interpreted as a constant potential, leaves the wave functions and the charge density unchanged. The same is also true for the kinetic and exchange-correlation energies. The Coulomb energy  $U\{n(\mathbf{r})\}$  changes by

$$\Delta U = V_0 \left[ \int d\mathbf{r} n(\mathbf{r}) - \sum_i Z_i \right] \quad (8)$$

since the potential acts also on the nuclear charges  $Z_i$ . By considering that the Fermi level is also shifted by  $V_0$ , we obtain for the change of  $\tilde{E}$

$$\Delta \tilde{E} = V_0 \left[ N - \sum_i Z_i \right], \quad (9)$$

which vanishes for a neutral (impurity plus host) system. Thus one sees that the grand-canonical functional  $\tilde{E}$  must be used. Otherwise the result would critically depend on the arbitrary choice of the zero-energy level, except when charge neutrality can be satisfied exactly.

### C. Single-particle energies and Lloyd's formula

With the help of the Kohn-Sham equations for the trial potential  $V_{\text{eff}}(\mathbf{r})$ , the kinetic energy is replaced by the

single-particle energies  $\epsilon_i$ , leading to the following decomposition of the total energy  $\tilde{E}$  into single-particle ( $E_{\text{s.p.}}$ ) and double-counting ( $E_{\text{DC}}$ ) contributions.

$$\tilde{E}\{n(\mathbf{r})\} = E_{\text{s.p.}} + E_{\text{DC}} \quad (10)$$

$$\begin{aligned} E_{\text{s.p.}} &= \sum_i \epsilon_i - E_F \left[ \int n(\mathbf{r}) d\mathbf{r} - N \right] \\ &= E_F N + 2 \int^{E_F} d\epsilon (\epsilon - E_F) n(\epsilon) \\ &= E_F N - 2 \int^{E_F} d\epsilon N(\epsilon). \end{aligned} \quad (11)$$

Here  $n(\epsilon)$  is the density of states and  $N(\epsilon)$  the integrated density of states per spin direction,

$$n(\epsilon) = -\frac{1}{\pi} \int d\mathbf{r} \text{Im} G(\mathbf{r}, \mathbf{r}; \epsilon), \quad N(E) = \int^E d\epsilon n(\epsilon). \quad (12)$$

The double-counting terms are given by

$$E_{\text{DC}} = - \int n(\mathbf{r}) V_{\text{eff}}(\mathbf{r}) d\mathbf{r} + U\{n(\mathbf{r})\} + E_{\text{xc}}\{n(\mathbf{r})\} \quad (13)$$

and will be discussed in the next subsection.

The energy integration for the single-particle energies can also be transformed into a contour integral due to the analytical properties of the Green's function:

$$E_{\text{s.p.}} = E_F N - \frac{2}{\pi} \text{Im} \oint dz (z - E_F) \int d\mathbf{r} G(\mathbf{r}, \mathbf{r}; z). \quad (14)$$

In the case of a point defect in an otherwise ideal crystal one needs the change  $\Delta n(\epsilon)$  of the density of states due to the defect and the change  $\Delta N(\epsilon)$  of the integrated density of states. This change can be calculated by either a shell-by-shell summation of the changes of the local densities of states or more elegantly by the formula given by Lloyd<sup>8</sup> and Lehmann.<sup>9</sup> In this formula, representing a generalization of the Friedel sum rule to multiple-scattering problems, the real-space integration has been performed analytically, resulting in

$$\begin{aligned} \Delta N(E) &= \frac{1}{\pi} \sum_{n,L} [\delta_n^L(E) - \delta_n^L(E)] \\ &\quad - \frac{1}{\pi} \text{Im} \ln \text{Det} |\delta_{nn'} \delta_{LL'} - \hat{G}_{LL'}^{nn'}(E) \Delta t_{l'}^{n'}(E)|. \end{aligned} \quad (15)$$

Here  $\delta_n^L(E)$  denotes the phase shifts for the  $n$ th muffin-tin potential.

In order to evaluate the single-particle energies by a contour integral in the complex energy plane, we need an analytical continuation of  $\Delta N(E)$  for complex energies  $z$  with no poles on the physical sheet. This is no problem for the second part in Eq. (15) describing the multiple-scattering contribution since here only the structural Green's functions and the  $t$  matrices enter, both of which have the proper analytical behavior. However, this is a problem for the phase-shift function  $\delta_l(E)$ , the analytical continuation of which indeed has poles on the physical sheet. This is most easily seen in the case of resonance scattering where the derivative  $d\delta_l/dE$  represents a Lorentzian,

$$\frac{1}{\pi} \frac{d\delta_l}{dE} \cong \frac{1}{\pi} \frac{\Gamma}{(E - E_0)^2 + \Gamma^2}, \quad (16)$$

which has simple poles  $z = E_0 \pm i\Gamma$  on both sides of the real axis, i.e., also on the physical sheet. In the Appendix we will derive a generalization of Lloyd's formula which has the desired analytical properties on the physical sheet. The result is

$$\begin{aligned} \Delta N(E) = & \frac{1}{\pi} \sum_{n,L} \text{Im} \ln \frac{\alpha_l^n(E)}{\hat{\alpha}_l^n(E)} \\ & - \frac{1}{\pi} \text{Im} \ln \text{Det} |\delta_{nn'} \delta_{LL'} - \hat{G}_{LL'}^{nn'}(E) \Delta t_l^{n'}(E)|. \end{aligned} \quad (17)$$

The basic idea in deriving this formula was to write the phase shift  $\delta_l^n(E)$  as the imaginary part of a complex quantity  $\ln \alpha_l^n(E)$  which for complex energies has the desired analytical properties, just as the density of states is related to the imaginary part of the Green's function. The coefficients  $\alpha_l^n(z)$  are determined by the behavior of the regular solution  $R_l^n(r, z)$  at the origin,

$$R_l^n(r, z) \cong \alpha_l^n(z) j_l(\sqrt{z}r) \quad \text{for } r \rightarrow 0, \quad (18)$$

and describe the enhancement over the potential-free solution  $j_l(\sqrt{z}r)$  at  $r=0$ . For real energies they are also directly connected with the phase shifts  $\delta_l^n(E)$  by the relation

$$\alpha_l^n(E) = |\alpha_l^n(E)| e^{i\delta_l^n(E)}, \quad (19)$$

which guarantees that the generalized Lloyd formula (17) is identical with the original one (15) on the real axis.

$$\begin{aligned} V_L^n(r) = & -\delta_{L0} \frac{Z^n}{r} + \frac{4\pi}{2l+1} \left[ \int_0^r dr' \frac{r'^{l+2}}{r^{l+1}} n_L^n(r') + \int_r^{R_{\text{WS}}} dr' \frac{r^l}{r'^{l-1}} n_L^n(r') \right] \\ & + (-r)^l \sum_{n' (\neq n)} \left[ A_L^{nn'} Z^{n'} + \sum_{L'} B_{LL'}^{nn'} \int_0^{R_{\text{WS}}} dr' r'^{l'+2} n_{L'}^{n'}(r) \right], \end{aligned} \quad (23)$$

where the constants  $A_L^{nn'}$  and  $B_{LL'}^{nn'}$  are given by

$$\begin{aligned} A_L^{nn'} &= \frac{4\pi}{2l+1} \frac{1}{|\mathbf{R}^n - \mathbf{R}^{n'}|^{l+1}} Y_L(\mathbf{R}^n - \mathbf{R}^{n'}), \\ B_{LL'}^{nn'} &= \frac{(4\pi)^2}{(2l+1)!!(2l'+1)!!} \\ &\times \sum_{L''} \delta_{l'', l'+l} C_{L''LL'} \frac{(2l''-1)!!}{|\mathbf{R}^n - \mathbf{R}^{n'}|^{l''+1}} \\ &\times Y_{L''}(\mathbf{R}^n - \mathbf{R}^{n'}), \end{aligned} \quad (24)$$

and  $C_{LL'L''}$  are Gaunt coefficients. The Madelung potential  $V_M(\mathbf{R}^n)$  follows directly from (23) by disregarding the first term, i.e., the self-interaction. For  $r \rightarrow 0$  only the angular momentum  $l=0$  contributes to the Madelung po-

#### D. Coulomb and exchange-correlation energies

The evaluation of the double-counting corrections (13) essentially requires the calculation of the Coulomb and exchange-correlation energies. The Coulomb energy  $U\{n(\mathbf{r})\}$  can be written as<sup>17</sup>

$$U = \frac{1}{2} \left[ \int d\mathbf{r} n(\mathbf{r}) V_c(\mathbf{r}) - \sum_n Z^n V_M(\mathbf{R}^n) \right]. \quad (20)$$

Here  $V_c(\mathbf{r})$  is the electrostatic potential which a test electron at position  $\mathbf{r}$  experiences in the field of all electrons and all nuclei. The Madelung potential  $V_M(\mathbf{R}^n)$  is identical with  $V_c(\mathbf{R}^n)$ , except that the diverging interaction with the nucleus at position  $\mathbf{R}^n$  is left out (no self-interaction). In cell-centered coordinates, where  $\mathbf{r}$  and  $\mathbf{r}'$  are vectors in the Wigner-Seitz cell, the electrostatic potential  $V_c^n(\mathbf{r})$  in the  $n$ th cell is given by

$$\begin{aligned} V_c^n(\mathbf{r}) = & \sum_{n'} \int_{\text{WS}} d\mathbf{r}' \frac{n^{n'}(\mathbf{r}')}{|\mathbf{r} - \mathbf{r}' + \mathbf{R}^n - \mathbf{R}^{n'}|} \\ & - \sum_{n'} \frac{Z^{n'}}{|\mathbf{r} + \mathbf{R}^n - \mathbf{R}^{n'}|}. \end{aligned} \quad (21)$$

For the evaluation of (20) and (21) we use a multipole expansion for the potential and the charge density in each cell,

$$V_c^n(\mathbf{r}) = \sum_L V_L^n(r) Y_L(\mathbf{r}), \quad n^n(\mathbf{r}) = \sum_L n_L^n(r) Y_L(\mathbf{r}), \quad (22)$$

and replace all integrals over Wigner-Seitz cells by integrals over Wigner-Seitz spheres with radius  $R_{\text{WS}}$ . After some algebra this leads to

potential. The spherically symmetric part  $V_{l=0}^n(r)$  is also required for the trial potential  $V_{\text{eff}}$  in the Kohn-Sham equations.

The largest contribution in the Coulomb energy arises from the intracell electron-nucleus interaction given by

$$- \sum_n Z^n \int_{\text{WS}} d\mathbf{r} \frac{n^n(\mathbf{r})}{r}. \quad (25)$$

This term, however, exactly cancels against the same term arising from the effective potential  $V_{\text{eff}}$  in (13). Therefore, the numerical accuracy can be increased if one introduces modified potentials  $\tilde{V}_{\text{eff}}(\mathbf{r})$ ,  $\tilde{V}_c(\mathbf{r})$ , and  $\tilde{V}_M(\mathbf{R}^n)$  such that the intracell electron-nucleus interaction is excluded.<sup>17</sup> The double-counting energy (13) is then given

by

$$E_{\text{DC}} = - \int d\mathbf{r} n(\mathbf{r}) \bar{V}_{\text{eff}}(\mathbf{r}) + \frac{1}{2} \left[ \int d\mathbf{r} n(\mathbf{r}) \bar{V}_c(\mathbf{r}) - \sum_n Z^n \bar{V}_n(\mathbf{R}^n) \right] + E_{\text{xc}}\{n(\mathbf{r})\}. \quad (26)$$

The exchange-correlation energy in the local-density approximation is given by

$$E_{\text{xc}}\{n(\mathbf{r})\} = \int d\mathbf{r} n(\mathbf{r}) \epsilon_{\text{xc}}(n(\mathbf{r})). \quad (27)$$

Similar to the Coulomb energy we also calculate  $E_{\text{xc}}$  using the full, i.e., nonspherically symmetric, charge densities. In each cell we expand the energy  $\epsilon_{\text{xc}}(n^n(\mathbf{r}))$  into spherical harmonics, yielding  $r$ -dependent coefficients  $\epsilon_{\text{xc}L}^n(r)$ . The total exchange-correlation energy is then given by

$$E_{\text{xc}} = \sum_{n,L} \int_0^{R_{\text{ws}}} r^2 dr n_L^n(r) \epsilon_{\text{xc}L}^n(r). \quad (28)$$

The xc coefficients  $\epsilon_{\text{xc}L}^n(r)$  are evaluated by a Gauss integration with weighting coefficients  $w_i$ :<sup>18</sup>

$$\epsilon_{\text{xc}L}^n(r) = \int d\Omega Y_L(\Omega) \epsilon_{\text{xc}}(n^n(r, \Omega)) \cong \sum_{i=1}^N w_i Y_L(\Omega_i) \epsilon_{\text{xc}}(n^n(r, \Omega_i)). \quad (29)$$

Detailed calculations show that an accuracy sufficient for all practical purposes can be achieved with 72 mesh points  $\Omega_i$ . A similar integral is also needed for the exchange-correlation potential entering  $V_{\text{eff}}$ . Here only the spherically symmetric  $l=0$  term is required.

### III. TEST CALCULATIONS FOR V IMPURITIES IN Cu

In this section we present test calculations for V impurities in Cu in order to demonstrate the convergence of the calculations with respect to two important parameters: (i) the number of perturbed shells of Cu atoms taken into account in the calculation, and (ii) the maximum angular momentum  $l_{\text{max}}$  used in the expansion of the wave functions and the Green's functions, respectively.

Table I lists the result for the shell convergence. First, the solution energy  $E_s$  (See Sec. IV) has been calculated in the single-site approximation where only the impurity potential is calculated self-consistently and all host potentials are fixed to their ideal-crystal values. Then successively the potentials of the first shell of atoms, the first

two shells, the first three shells, and finally the first four shells are added to the calculation and determined self-consistently. In all these calculations a maximal angular momentum  $l_{\text{max}}=3$  has been used. From Table I one sees that the convergence is practically complete, once the potentials of the nearest neighbors, i.e., the first shell, are determined self-consistently. This is, however, only true if Lloyd's formula (17) is used to calculate the single-particle energies. If they are calculated by summing the shell-by-shell contributions to the local densities of states explicitly, the convergence is very slow and clearly not completed after four shells. The difference between these calculations is that in Lloyd's formula all changes of the local densities of states over the infinite crystal volume have been summed implicitly. The extremely good convergence obtained by Lloyd's formula can be explained by the frozen-potential theorem.<sup>19</sup> Under frozen-potential conditions, if, e.g., only the potentials of the impurity and the first-shell atoms are relaxed, but all others are frozen to their ideal-crystal values, the changes of the total energy due to the perturbed density of states and charge densities in the "outer" region are given in first order by the single-particle energies alone, which are correctly evaluated using Lloyd's formula.

Test calculations for the angular-momentum convergence are shown in Table II. In solving the radial Schrödinger equation and the Dyson equation (3), an angular-momentum cutoff of  $l_{\text{max}}=2, 3$ , and 4 has been used. One shell of perturbed potentials is included and the single-particle energies are calculated using Lloyd's formula. The angular-momentum convergence is relatively slow, and  $l_{\text{max}}=2$  is clearly not sufficient.

Finally, we have tested the angular-momentum expansion for the charge density which is necessary to evaluate the Coulomb and exchange-correlation energies. We found that a maximal angular momentum  $l'_{\text{max}}=4$  is sufficient for a reliable calculation of these energies. The nonsphericity of the charge density can have an important effect on the total energy. In the case of V in Cu the resulting solution energy is 0.80 eV, i.e., 0.21 eV too high, if the nonspherical components of the charge density are neglected in evaluating the double-counting energies.

### IV. SOLUTION ENERGIES OF 3d IMPURITIES IN Cu and Ni

In this section we present results for solution energies of 3d impurities in Cu and Ni. They were calculated using maximum angular momenta  $l_{\text{max}}=4$  for the Green's

TABLE I. Test of the shell convergence for a V impurity in Cu. In the calculation successively only the impurity potential [single-site (SS)] and then one shell, two shells, three shells, and four-shells of neighboring potentials were allowed to relax and be calculated self-consistently. A maximum angular momentum  $l_{\text{max}}=3$  was used. Two ways of estimating the single-particle energies (Lloyd's formula and local summation) are listed. Given are the solution energies for V in Cu in eV/atom.

$E_s$ (eV)	SS	One shell	Two shells	Three shells	Four shells
Lloyd	1.4433	0.7299	0.7300	0.7298	0.7303
Local summation	1.6043	1.9253	1.3810	0.7520	0.5178

TABLE II. Test of the angular-momentum convergence for a V impurity in Cu. The results for the solution energy for V in Cu are listed as a function of the maximal angular momentum  $l_{\max}$  used in evaluating the Green's function. The calculation refers to one shell of perturbed potentials and the use of Lloyd's formula for the single-particle energies.

	$l_{\max}=2$	$l_{\max}=3$	$l_{\max}=4$
$E_s$ (eV)	1.10	0.73	0.59

functions and  $l'_{\max}=6$  for the charge density in the double-counting terms. The perturbed potentials on the nearest-neighbor atoms are calculated self-consistently, with the potentials of all other shells being unrelaxed. As was demonstrated in the preceding section, this is sufficient for a reliable calculation of solution energies. The formation energy of a binary alloy  $A_{1-c}B_c$ , where  $c$  is the atomic concentration of  $B$  atoms, is defined by

$$E(c) = E_{A_{1-c}B_c} - (1-c)E_A - cE_B. \quad (30)$$

Here  $E_{A_{1-c}B_c}$  is the total energy of the alloy averaged over all possible configurations.  $E_A$  and  $E_B$  are the energies of the pure metals. The solution energy  $E_s^B$  in  $A$  is given by derivative  $dE/dc$  in the dilute limit  $c \rightarrow 0$ :

$$E_s^B \text{ in } A = \Delta E_{AB} - E_B + E_A \quad (31)$$

with  $\Delta E_{AB} = \left. \frac{d}{dc} E_{A_{1-c}B_c} \right|_{c=0}$ .

$\Delta E_{AB}$  is the energy difference between an  $A$  crystal with a substitutional  $B$  impurity and the pure  $A$  crystal. This is the central quantity to be calculated. The ideal-crystal values  $E_A$  and  $E_B$  are evaluated by self-consistent augmented-spherical-wave (ASW) band-structure calculations.<sup>20</sup>

The results for  $3d$  impurities in Cu are listed in Table III and shown in Fig. 1. We have performed both spin-polarized and non-spin-polarized (paramagnetic) calculations. The differences are quite important and are due to the large local moment of these impurities. (As far as the electronic structure and the local moments are concerned, the present results are practically identical to the ones given by Braspenning *et al.*<sup>2,3</sup>) The largest magnetic reduction (0.7 eV) is obtained for Mn, which also has the largest moment ( $3.4\mu_B$ ) in the  $3d$  series.<sup>3</sup> The magnetic effects for the hosts are smaller and not so important. (For Mn the ASW band-structure calculation for

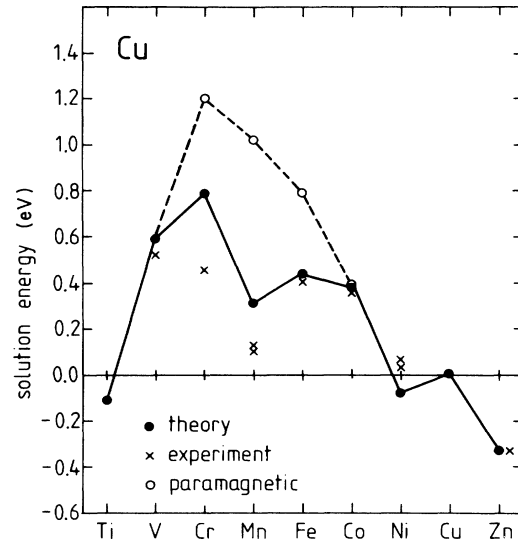


FIG. 1. Solution energies of  $3d$  impurities in Cu (●, spin-polarized calculation; ○, paramagnetic calculation; ×, experimental values).

the host refers to a nonmagnetic fcc structure; an antiferromagnetic calculation for the actual ground-state structure is not available.) By comparing with the experimental data we see that the calculations reproduce the experimental trends quite well. In particular, the minimum for Mn, being purely of magnetic origin, shows up well. Nevertheless, the differences for Mn and Cr are sizable. Part of this might be due to lattice relaxations, which would lower the energy, but have been neglected in our calculations. One would expect them to be most important for the early  $3d$  impurities.

Table III also includes the values calculated from Miedema's empirical formula.<sup>13</sup> In agreement with the well-known success of Miedema's parametrization, these values are of similar quality as our *ab initio* results. It is especially amazing to see that the strong reduction for Mn is given so well by Miedema's model, despite the fact that the magnetism is included only very indirectly in this approach.

Table IV and Fig. 2 show analogous results for  $3d$  impurities in Ni. The electronic and magnetic structure of  $3d$  impurities in Ni has been recently calculated by us<sup>21,22</sup>

TABLE III. Solution energies of  $3d$  impurities in Cu. The central results are the values given by the spin-polarized calculation. Also included are the results of a paramagnetic calculation and the spin-polarized results in the single-site approximation. Miedema's values are taken from Ref. 13.

$E_s$ (eV)	Ti	V	Cr	Mn	Fe	Co	Ni	Cu	Zn
Spin pol.	-0.11	0.59	0.79	0.31	0.44	0.38	-0.08	0	-0.33
Paramagnetic	-0.11	0.59	1.20	1.02	0.79	0.39	-0.08	0	-0.33
Single site (spin pol.)	0.89	1.30	1.23	0.60	0.55	0.36	-0.10	0	-0.26
Experiment	-2.5 <sup>a</sup>	0.52 <sup>b</sup>	0.45 <sup>a</sup>	0.12 <sup>a</sup>	0.41 <sup>a</sup>	0.40 <sup>a</sup>	0.06 <sup>b</sup>	0	-0.34 <sup>a</sup>
				0.1 <sup>c</sup>	0.40 <sup>c</sup>	0.35 <sup>c</sup>	0.03 <sup>c</sup>	0	
Miedema	-0.80	+0.17	+0.54	+0.15	+0.62	+0.36	+0.27	0	-0.32

<sup>a</sup>Reference 4.

<sup>b</sup>Reference 27.

<sup>c</sup>Reference 28.

TABLE IV. Solution energies of 3*d* impurities in Ni.

$E_s$ (eV)	Ti	V	Cr	Mn	Fe	Co	Ni	Cu	Zn
Spin pol.	-1.86	-1.21	-0.25	-0.54	-0.58	-0.19	0	0.20	-0.54
Single site	-1.22	-0.33	0.26	-0.25	-0.30	-0.16	0	0.18	-0.45
Experiment			-0.10 <sup>a</sup>	-0.56 <sup>a</sup>	-0.22 <sup>a</sup>	0.00 <sup>a</sup>	0	0.10 <sup>a</sup>	-0.38 <sup>b</sup>
						0.09 <sup>b</sup>		0.12 <sup>b</sup>	
Miedema	-1.76	-0.78	-0.27	-0.34	-0.06	-0.01	0	+0.27	-0.84

<sup>a</sup>Reference 4.<sup>b</sup>Reference 27.

and will not be repeated here. The agreement with the experimental data is satisfactory. Only for Fe in Ni does a larger discrepancy occur. Here also Miedema's parametrization accounts well for the experimental data.

An important difference between the Cu and Ni results can clearly be seen from Figs. 1 and 2. Whereas all 3*d* impurities, with the exception of Ni and Ti, have an endothermic solubility in Cu, their solubility in Ni is strongly exothermic. The basic difference is the strong hybridization between the impurity *d* electrons and the *d* electrons of Ni, which is to a large extent absent in Cu due to the stronger localization of the *d* electrons. As a typical example, we want to discuss the situation for V impurities, which, according to our results, have a solution energy of +0.59 eV in Cu, but -1.21 eV in Ni. Thus the solution energies differ by 1.80 eV. These differences are also reflected in the local densities of states of the V impurities in the Cu and Ni host, which are shown in Fig. 3. In Cu essentially two features can be seen: some hybridized intensity within the range of the Cu *d* band between -6 and -2 eV, and the virtual bound states around the Fermi energy which have a half-width of about 2 eV. Due to the hybridization with the *d* electrons of Cu, as well as due to the hybridization with the *sp* electrons leading to the broadening of the virtual bound states, some energy is gained. However, this ener-

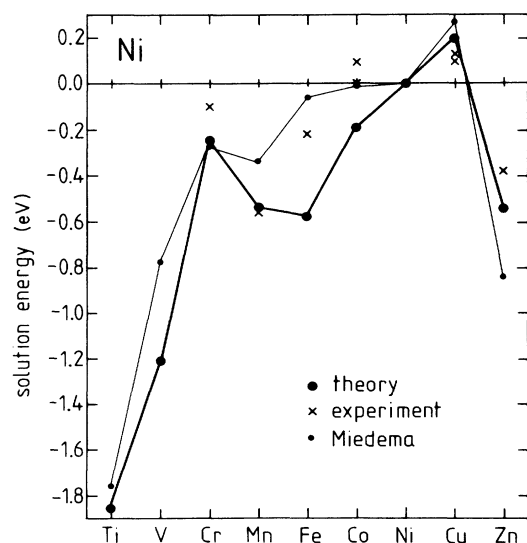


FIG. 2. Solution energies of 3*d* impurities in Ni (● spin-polarized calculation; ●, Miedema's values; ×, experimental results).

gy gain is not sufficient to overcome the lost cohesion of the pure metals. For the Ni-host, on the other hand, the situation is much more favorable. Due to the stronger hybridization with the *d* electrons of Ni, the genuine virtual bound states are pushed completely above the Fermi energy and only Ni-like *d* states are occupied. Since the empty virtual bound states have antibonding character, whereas the occupied hybrids in the Ni *d* band are bondinglike, this strongly favors the formation of V impurities in Ni and explains the large negative solution energies. This situation just corresponds to the half-filled *d* band in the transition-metal series, for which the cohesion energy is maximal.

Finally, we want to briefly comment on the validity of the single-site approximation, i.e., when the nearest-neighbor potentials are assumed to be unperturbed and only the impurity potential is calculated self-consistently. This is interesting in connection with concentrated disordered alloys where, due to the many configurations involved, cluster-type calculations such as the present ones are very difficult. Here the most successful theory is the KKR CPA,<sup>23</sup> which relies on a single-site approximation. In the dilute limit, a self-consistent KKR CPA calculation should be in agreement with the single-site values listed in Tables I and II. From the data we see that the single-site approximation works fairly well only as long as the valence difference is sufficiently small. For large  $\Delta Z$  differences, charge-transfer effects, etc. become important and the single-site approximation yields unreliable results. For example, for V impurities this approximation is in error by 0.9 eV for the Ni host and 0.7 eV for Cu. Similar errors are therefore also to be expected in KKR CPA calculations for such concentrated alloys. In this connection we refer to recent results for dilute Cu-Pd alloys<sup>24</sup> for which KKR CPA calculations<sup>25</sup> lead to considerable errors.

## V. SUMMARY AND CONCLUSIONS

In this paper we have presented a formalism to calculate total energies for point defects in metals which is suitable for the KKR Green's-function method. For this purpose we have introduced a grand-canonical energy functional which is extremal against non-particle-conserving charge-density variations. We have given an extension of Lloyd's formula for the integrated density of states, which allows one to calculate the single-particle energies by the complex energy method. The wave functions and charge densities are constructed by spherically symmetric atomic-sphere potentials. However, the full

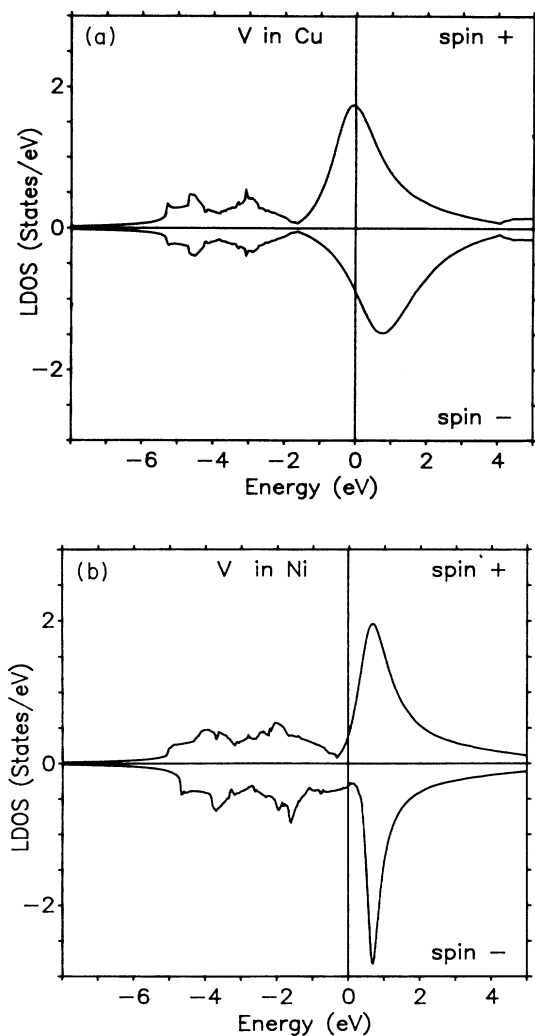


FIG. 3. Local densities of states for V impurities in Cu and Ni. Plotted are the local densities of states in the impurity Wigner-Seitz sphere for both spin directions.

nonspherical charge densities are taken into account in the total-energy calculation.

Test calculations for V impurities in Cu show that for a calculation of impurity solution energies it is sufficient to include angular momenta up to  $l_{\max}=4$  and one shell of perturbed host potentials around the impurity. Extensive calculations for the solution energies of  $3d$  impurities in Cu and Ni show good agreement with the experimental data and with Miedema's approach. Large magnetic effects occur in the middle of the  $3d$  series, especially for Mn. In general, we obtain an endothermic solubility in Cu, but an exothermic solubility in Ni. This difference arises mostly from the different role of impurity  $d$ -host  $d$  hybridization in these hosts.

The present calculations completely neglect lattice relaxations around the impurity, which would lower the calculated solution energy. The present results (Fig. 1) indicate that this may be important for the early transition-metal impurities in Cu and Ni. Therefore it would be desirable to include such size effects in future

calculations.

*Note added.* As has been shown in Sec. II B and in the Appendix, the Friedel formula, Eqs. (15) and (A10), cannot be used for complex energies since the phase-shift function  $\delta_l(E)$  does not have the proper analytical properties. Instead, one might think that the replacement of

$$\Delta N(E) = \frac{1}{\pi} \sum_L [\delta_l(E) - \delta_l(E)]$$

by

$$\Delta N(E) = \text{Im} \frac{1}{\pi} \sum_L \ln[t_l(E)/t_l(E)]$$

would solve this problem since both expressions agree on the real axis and the  $t$  matrix  $t_l(z)$  is analytic for complex  $z$  values. However, this is not the case because of possible zeros of the  $t$  matrix  $t_l(E)$  resulting in additional branch points for  $\ln t_l(E)$ . As a result of such branch points, one can end up on the wrong sheet if contour integration is applied. Unfortunately, zeros of  $t_l(E)$  actually occur; e.g., for transition metals the  $s$ -phase shift changes sign within the valence-band region. Thus the straightforward use of the  $t$  matrix is incorrect. In contrast, Eq. (17), derived in the Appendix, is a generalization of Lloyd's formula for complex energies that has the correct analytical properties and guarantees that one always remains on the physical sheet. One of us (P.H.D.) would like to thank A. Gonis for clarifying discussions concerning this point.

#### ACKNOWLEDGMENTS

We would like to thank J. Deutz and H. Akai for their cooperation and for many discussions during the early stage of this work. We acknowledge support from North Atlantic Treaty Organization Collaborative Research Grant No. 0086/88. One of us (M.W.) was supported in part by the Alexander von Humboldt Foundation and by the Division of Materials Sciences, U.S. Department of Energy (Contract No. DE-AC02-76CH00016).

#### APPENDIX: LLOYD'S FORMULA FOR COMPLEX ENERGIES

The generalized Lloyd formula of Eq. (17) and the standard one, Eq. (15), differ only in the single-site terms. Therefore we consider here only the scattering at a single muffin-tin potential. For a given angular momentum  $l$ , the change  $\Delta n_l(E)$  of the density of states due to a spherically symmetric muffin-tin potential is, according to Eqs. (1) and (4), given by

$$\Delta n_l(E) = -\frac{1}{\pi} \text{Im} \Delta G_l(E), \quad (\text{A1})$$

with

$$\Delta G_l(E) = \lim_{R \rightarrow \infty} \sqrt{E} \int_0^R r^2 dr [H_l(r; E) R_l(r; E) - h_l(\sqrt{E}r) j_l(\sqrt{E}r)]. \quad (\text{A2})$$

Instead of taking the imaginary part in Eq. (A2) directly, which would lead to the replacement of  $H_l$  and  $h_l$  by  $R_l$  and  $j_l$ , we will evaluate  $\Delta G_l(z)$  for complex energies  $z$  since this quantity is essentially the difference of two

Green's functions; as such, it is analytical on the whole physical sheet with the exception of the real axis.

The integration over the radius can be performed analytically as we will show below:

$$\int_0^R r^2 dr H_l(r; z) \dot{R}_l(r; z) = r^2 [H_l'(r; z) \dot{R}_l(r; z) - H_l(r; z) \dot{R}_l'(r; z)] \Big|_{r=0}^{r=R}. \quad (\text{A3})$$

Here the prime means a derivative with respect to  $r$ , and the overdot an energy derivative. Close to the origin,  $R_l(r; z)$  and  $H_l(r; z)$  behave as

$$\begin{aligned} R_l(r; z) &\cong \alpha_l(z) j_l(\sqrt{z}r), \\ H_l(r; z) &\cong \frac{1}{\alpha_l(z)} h_l(\sqrt{z}r) \quad \text{for } r \rightarrow 0. \end{aligned} \quad (\text{A4})$$

The reciprocal "enhancement" of the regular and nonregular solutions at the origin follows from the Wronsky relation

$$H_l'(r; z) R_l(r; z) - H_l(r; z) R_l'(r; z) = \frac{1}{\sqrt{z}r^2},$$

which is also valid for the potential-free solutions  $j_l$  and  $h_l$ . For large  $r$  values we can use the asymptotic formulas of Eq. (2) for  $R_l$  and  $H_l$ . Taking everything together we obtain for  $\Delta G_l(z)$

$$\begin{aligned} \Delta G_l(z) &= -\frac{\dot{\alpha}_l(z)}{\alpha_l(z)} \\ &+ \lim_{R \rightarrow \infty} z \Delta t_l(z) R^2 [h_l'(\sqrt{z}R) \dot{h}_l(\sqrt{z}R) - h_l \dot{h}_l']. \end{aligned} \quad (\text{A5})$$

Using the asymptotic formula for  $h_l$ ,

$$h_l(\sqrt{z}R) \approx -\frac{1}{\sqrt{z}R} e^{i(\sqrt{z}R - l\pi/2)} \quad \text{for } R \rightarrow \infty, \quad (\text{A6})$$

we see that the last term in Eq. (A5) decreases exponentially on the whole physical sheet, i.e., for  $\text{Im } \sqrt{z} > 0$ . Therefore, in the limit  $R \rightarrow \infty$  this term gives no contribution. This is also true when approaching the real axis, which means  $z = E + i\epsilon$  with  $\epsilon \rightarrow 0+$ . Note that the limit

$\epsilon \rightarrow 0+$  has to be performed after the limit  $R \rightarrow \infty$ . Therefore we obtain for  $\Delta G_l$  of Eq. (A2),

$$\Delta G_l(E) = -\frac{\dot{\alpha}_l(E)}{\alpha_l(E)} = -\frac{d}{dE} \ln \alpha_l(E), \quad (\text{A7})$$

and for the integrated density of states for real energies,

$$\Delta N_l(E) = -\frac{1}{\pi} \text{Im} \Delta G_l(E) = \frac{1}{\pi} \text{Im} \ln \alpha_l(E), \quad (\text{A8})$$

which directly leads to the generalized Lloyd's formula (17). That Eq. (19) connects the  $\alpha_l(E)$  coefficients with the phase shifts  $\delta_l(E)$  can be seen as follows: For real energies the regular solution can be written as a phase factor  $e^{i\delta_l(E)}$  times a real function  $\tilde{R}_l(r; E)$ ,

$$R_l(r; E) = e^{i\delta_l(E)} \tilde{R}_l(r; E). \quad (\text{A9})$$

With  $\alpha_l(E)$  defined by (A4) then, at the origin we obtain the relation  $\alpha_l = |\alpha_l| e^{i\delta_l}$  from which the usual form of the Friedel sum rule follows:

$$\Delta N_l(E) = \frac{1}{\pi} \delta_l(E). \quad (\text{A10})$$

We still have to prove Eq. (A3). For this we take the energy derivative of the radial Schrödinger equation for  $R_l(r; z)$  which yields

$$\left[ -\frac{1}{r} \partial_r^2 r + \frac{l(l+1)}{r^2} + V(r) - z \right] \dot{R}_l(r; z) = R_l(r; z). \quad (\text{A11})$$

Multiplying this equation by  $H_l(r, z)$  and subtracting from this the Schrödinger equation for  $H_l(r; z)$  multiplied by  $\dot{R}_l(r, z)$  we obtain

$$\begin{aligned} H_l(r; z) R_l(r; z) &= H_l(r; z) \left[ -\frac{1}{r} \partial_r^2 r \right] \dot{R}_l(r, z) \\ &- \dot{R}_l(r, z) \left[ -\frac{1}{r} \partial_r^2 r \right] H_l(r; z). \end{aligned} \quad (\text{A12})$$

By taking the volume integral as in (A3), we can integrate the right-hand site and obtain the desired result (A3).

- <sup>1</sup>G. F. Koster and J. C. Slater, Phys. Rev. **95**, 1167 (1954); G. A. Baraff and M. Schlüter, Phys. Rev. B **19**, 4965 (1979); J. Bernholc, N. O. Lipari, and S. T. Pantelides, *ibid.* **21**, 3545 (1980); C. Koenig, P. Leonard, and E. Daniel, J. Phys. (Paris) **42**, 1015 (1981).  
<sup>2</sup>R. Podloucky, R. Zeller, and P. H. Dederichs, Phys. Rev. B **22**, 5777 (1980).  
<sup>3</sup>P. J. Braspenning, R. Zeller, A. Lodder, and P. H. Dederichs, Phys. Rev. B **29**, 730 (1984).  
<sup>4</sup>O. Gunnarsson, O. Jepsen, and O. K. Andersen, Phys. Rev. B **27**, 7144 (1983).  
<sup>5</sup>F. Gautier, G. Moraitis, and J. L. Parlebas, J. Phys. F **6**, 381 (1976); F. Gautier, J. van der Rest, and F. Brouers, J. Phys. F **5**, 1884 (1975).  
<sup>6</sup>A. Pasturel, P. Hicter, and F. Cyrot-Lackmann, Solid State

- Commun. **48**, 561 (1983).  
<sup>7</sup>J. C. Gachou, M. Notin, C. Cunat, J. Herz, J. L. Parlebas, G. Moraitis, B. Stupfel, and F. Gautier, Acta Metall. **28**, 489 (1980).  
<sup>8</sup>P. Lloyd, Proc. Phys. Soc. London **90**, 207 (1967); **90**, 217 (1967).  
<sup>9</sup>G. Lehmann, Phys. Status Solidi B **70**, 737 (1975).  
<sup>10</sup>C. König, J. Phys. F **3**, 1497 (1973).  
<sup>11</sup>R. Zeller, J. Deutz, and P. H. Dederichs, Solid State Commun. **44**, 993 (1982).  
<sup>12</sup>A. R. Williams, P. J. Feibelman, and N. D. Lang, Phys. Rev. B **26**, 5433 (1982).  
<sup>13</sup>A. R. Miedema, P. F. de Chatel, and F. R. de Boer, Physica B **100**, 1 (1980).  
<sup>14</sup>U. v. Barth and L. Hedin, J. Phys. C **5**, 1629 (1972).

- <sup>15</sup>V. R. Moruzzi, J. F. Janak, and A. R. Williams, *Calculated Electronic Properties of Metals* (Pergamon, New York, 1978).
- <sup>16</sup>N. D. Mermin, Phys. Rev. **137**, A1441 (1965); J. Deutz, R. Zeller, and P. H. Dederichs, Kernforschungsanlage Jülich Report No. 1805, 1982 (unpublished).
- <sup>17</sup>M. Weinert, E. Wimmer, and A. J. Freeman, Phys. Rev. B **26**, 4571 (1982).
- <sup>18</sup>M. Abramowitz and I. A. Stegun, *Handbook of Mathematical Functions* (Dover, New York, 1965).
- <sup>19</sup>D. G. Pettifor, Commun. Phys. **1**, 141 (1976); D. G. Pettifor and C. M. Varma, J. Phys. C **12**, L253 (1979); H. L. Skriver, Phys. Rev. Lett. **49**, 1768 (1982); M. Methfessel and J. Kübler, J. Phys. F **12**, 41 (1982).
- <sup>20</sup>A. R. Williams, J. Kübler, and C. D. Gelatt, Phys. Rev. B **19**, 6094 (1979).
- <sup>21</sup>R. Zeller, J. Phys. F **17**, 2123 (1987).
- <sup>22</sup>N. Stefanou, A. Oswald, R. Zeller, and P. H. Dederichs, Phys. Rev. B **35**, 6911 (1987).
- <sup>23</sup>G. M. Stocks, W. M. Temmerman, and B. L. Gyorffy, Phys. Rev. Lett. **41**, 339 (1978); H. Akai, J. Phys. Soc. Jpn. **51**, 468 (1982); H. Winter and G. M. Stocks, Phys. Rev. B **27**, 882 (1983).
- <sup>24</sup>N. Stefanou, R. Zeller, and P. H. Dederichs, Solid State Commun. **62**, 735 (1987); P. Weightman, H. Wright, S. D. Waddington, D. van der Marel, G. Sawatzky, G. P. Diakun, and D. Norman, Phys. Rev. B **36**, 9098 (1987).
- <sup>25</sup>H. Winter, P. J. Durham, W. M. Temmerman, and G. M. Stocks, Phys. Rev. B **33**, 2370 (1986).
- <sup>26</sup>P. Ziesche and G. Lehmann, *Ergebnisse in der Elektronentheorie der Metalle* (Springer-Verlag, Berlin, 1983).
- <sup>27</sup>O. Kubaschewsky and C. B. Alcock, *Metallurgical Thermochemistry* (Pergamon, Oxford, 1979).
- <sup>28</sup>R. Hultgren, P. D. Desai, D. T. Hawkins, M. Gleiser, and K. K. Kelly, *Selected Values of Thermodynamic Properties of Metals and Alloys* (American Society of Metals, Metals Park, OH, 1973).